CrossMark
click for updates

View Article Online
View Journal

NJC

Accepted Manuscript

This article can be cited before page numbers have been issued, to do this please use: J. Chen, Y. Chen, Y. Wu, X. Wang, Z. Yu, L. Xiao, Y. Liu, H. Tian, J. Yao and H. Fu, *New J. Chem.*, 2017, DOI: 10.1039/C6NJ02747D.

Volume 40 | Number 1 | January 2016 | Pages 1–846

NJC

New Journal of Chemistry
www.rsc.org/njc

A journal for new directions in chemistry

ISSN 1144-0546

ROYAL SOCIETY OF CHEMISTRY

PAPER
Jason B. Benedict *et al.*
The role of atropisomers on the photo-reactivity and fatigue of diarylethene-based metal–organic frameworks

cnrs

This is an Accepted Manuscript, which has been through the Royal Society of Chemistry peer review process and has been accepted for publication.

Accepted Manuscripts are published online shortly after acceptance, before technical editing, formatting and proof reading. Using this free service, authors can make their results available to the community, in citable form, before we publish the edited article. We will replace this Accepted Manuscript with the edited and formatted Advance Article as soon as it is available.

You can find more information about Accepted Manuscripts in the author guidelines.

Please note that technical editing may introduce minor changes to the text and/or graphics, which may alter content. The journal's standard Terms & Conditions and the ethical guidelines, outlined in our author and reviewer resource centre, still apply. In no event shall the Royal Society of Chemistry be held responsible for any errors or omissions in this Accepted Manuscript or any consequences arising from the use of any information it contains.

ROYAL SOCIETY OF CHEMISTRY

rsc.li/njc

View Article Online
DOI: 10.1039/C6NJ02747D

NJC

ARTICLE

Modulated Emission from Dark Triplet Excitons in Aza-Acene Compounds: Fluorescence Versus Phosphorescence

Received 00th January 20xx,
Accepted 00th January 20xx

DOI: 10.1039/x0xx00000x

www.rsc.org/

Jianwei Chen, [ab⊥] *Yi Chen,* [c⊥] *Yishi Wu **[a]*, Xuedong Wang,* [ab] *Zhenyi Yu,* [ab] *Lu Xiao,* [ab] *Yanping Liu,* [ab] *He Tian**[c] *, Jiannian Yao* [a] *and Hongbing Fu **[ad]

The interest in the field of organic light-emitting diodes (OLEDs) is how to make the optically dark triplet excitons shine in order to increase the electro-optic conversion efficiency of the devices. In this work, two kinds of phenazine compounds, i.e. dibenzo[a,c]phenazine (DBP) and tribenzo[a,c,i]phenazine (TBP), were synthesized and used as model compounds to regulate the emission efficiency of the dark triplet excitons by chemical modification. Charge-transfer induced ultrafast intersystem crossing (CT-ISC) with time constant of ~ 1 ps was observed for these two phenazine derivatives upon photoexcitation with high triplet yield of 77.1% for DBP and 58.7% for TBP. The triplet excited states of DBP can produce ultra-long phosphorescence with lifetime as long as 318 ms at 77 K. The quantum yield for phosphorescence (Φ_P) is determined to be 8.45%. In sharp contrast, the triplet-excited ^{3}TBP* undergoes efficient reverse intersystem crossing (RISC) process, resulting in bright delayed fluorescence emission with negligible phosphorescence. A controllable luminescence behavior from the triplet states between fluorescence and phosphorescence in phenazine derivatives is demonstrated. Theoretical calculations reveal that the structure-dependent triplet evolution is due to the charge-transfer induced energy level alignment within these compounds. Our results may have potential applications for the designing of OLEDs and high triplet yields pure organic materials.

1. Introduction

The organic luminescent materials have witnessed significant advance owing to their wide applications including latent fingerprints,[1] fluorescent probes,[2] biological imaging,[~~1-~~3] temperature sensor,[4-5] organic solid state lasers[6-9] and especially organic light-emitting diodes (OLEDs)[10-11]. Statistically, spin-independent injection of charge carriers forms about 25% singlet excitons and 75% triplet excitons in OLED devices. The utilization of triplet excitons to generate light has received considerable attention to exceed the predicted limitation for high performance OLED devices during the past decades.[12-17] One viable way is to use organic phosphorescent semiconducting materials. Highly efficient OLED devices have been developed using transition metal-containing organic complex systems such as Alq3, Ir(ppy)3, etc.[13, 18] Turning the non-radiative triplet states to the radiative singlet states via promoting the reverse intersystem crossing (RISC) process is certified to be another promising approach for high performance luminescence devices.[11,19] Thermal activated delayed fluorescence (TADF) has been achieved to enhance the luminescence of the OLEDs, giving rise to a quantum yield of more than 90%.[11]

Another kind of RISC process, which start from high-energy triplet states (T_n) and is called as the hot excition path in the previous publication,[20] should be drawn enough attention. This hot excition path RISC process has been found in several system such as anthracene derivatives,[21] organic dyes[22] and excited-state intramolecular proton transfer (ESIPT) materials.[23] Recently, Ma and co-workers successfully applied this process in the OLEDs device and harvested efficiency as high as 93%,[24] which strongly suggest that the hot excition path RISC process is an efficient way to transform the non-radiative triplet states to the radiative singlet states.

We here choose two benzophenazine(BP) derivatives, dibenzo[a,c]phenazine (DBP) and tribenzo[a,c,i]phenazine (TBP) (Fig. 1), as model triplet generating materials to explore the hot excition path RISC process for their charge-transfer induced high triplet efficiency and simple synthesis route. By appropriate molecular modification, the energy level structure of singlet and triplet manifold can be reorganized. As a result of the modulated energy level, different photophysical processes is demonstrated. DBP acts as a good phosphorescence emitter with emission lifetime as long as 318 ms at 77 K whereas TBP is shown to exhibit bright delayed fluorescence due to reverse intersystem crossing (RISC) from high-

---

[a] *Beijing National Laboratory for Molecular Sciences (BNLMS), Institute of Chemistry, Chinese Academy of Sciences, Beijing, 100190, China. E-mail: hongbing.fu@iccas.ac.cn; yswu@iccas.ac.cn.*
[b] *University of Chinese Academy of Sciences, Beijing, 100039, China.*
[c] *Key Laboratory for Advanced Materials and Institute of Fine Chemicals, East China University of Science & Technology, Shanghai 200237, P. R. China. E-mail: tianhe@ecust.edu.cn.*
[d] *Department of Chemistry, Capital Normal University, Beijing, 100048, China.*
[⊥] *These authors contributed equally.*

† Electronic Supplementary Information (ESI) available. See DOI: 10.1039/x0xx00000x

View Article Online
DOI: 10.1039/C6NJ02747D

energy triplet states (T_n) to lowest lying singlet state (S_1). These findings are meaningful for the development of high performance OLED devices and high triplet yields pure organic materials.

2. Experimental

2.1 Synthesis

The BP compounds were prepared by amination of phenanthrene-9, 10-dione via one pot reaction with yield of more than 80% according to the previous literature.[25] Details of the synthetic route were elaborated in the Electronic Supplementary Information (ESI). Both DBP and TBP were fully characterized with ^{1}HNMR, ^{13}CNMR and mass spectrometry (MS). All the chemical reagents and solvents used were purchased commercial sources and were of analytical grade.

2.2 Spectral measurements

The absorption spectra were recorded on a SHIMADZU UV-3600 spectrophotometer. The room-temperature emission spectra were recorded on a HORIBA Fluoromax-4NIR spectrophotometer. The luminescence spectra, phosphorescence spectra and the decay lifetime of phosphorescence at 77 K were recorded on a HITACHI F-7000 spectrophotometer with the low temperature attachment. The luminescence spectra contain not only the fluorescence spectra, but also the phosphorescence spectra. A chopper system, which includes two choppers and the rotating speed of these two choppers can be controlled by a computer, was used to differentiate fluorescence and phosphorescence. By regulating the rotating speed of chopper, short-lived photons were shielded by the leaf of the chopper while long-lived photons were allowed to pass through. The luminescence spectra were recorded at the normal mode, which allows all the radiant photons including short-lived fluorescence photons and long-lasting phosphorescence photons to pass through. The phosphorescence spectra were recorded at the chopper mode with the chopper rotating at the setting speed which only allows long-life photons to pass through. A streak camera system with a Ti:sapphire femtosecond laser system generating the pump pulses (800 nm, 130 fs, 1 kHz), the accuracy of which is 20 ps, was used to record the time-resolved fluorescence decay transient spectra. This system was also used to provide the pump pulses (413.8 uj/cm^2) and the probe pulses for the femtosecond ultrafast transient absorption system. The emission spectra of singlet oxygen were record on a Princeton Instruments IsoPlane 160 spectrophotometer with NIRvana ST 640 as the CCD. Details for the measurement of singlet oxygen yields were illustrated in the Result and discussion part.

2.3 Transient absorption spectroscopy

The femtosecond ultrafast transient absorption system is based on a two probe beam system passing through two different parts of the sample with one part of the sample excited by the pump beam. Thus, we can calculate the absorbance difference for these two probe beams to obtain the absorption spectra of the excited-states. Details for this system have been published previously.[26] The nanosecond flash photolysis signals were detected on the Edinburgh LP920 and record on the Tektronix TDS 3012B oscilloscope and computer.

2.4 Quantum chemical calculations

All theoretical calculations were executed by the Gaussian 09 software package.[27] The ground states of the BP compounds were calculated by the density functional theory (DFT) method and the excited states were calculated by the time-dependent density functional theory (TD-DFT) method. For all atoms, the geometries of molecules were optimized at the B3LYP/6-311^{++}G** level in the gas phase. The isosurface upon the $S_0 \rightarrow S_n$ and $S_0 \rightarrow T_n$ transitions were carried out using the Multiwfn software.[28]

3. Results and discussion

3.1. Basic spectral characterization

The phenazine derivatives, which belong to the N-heteroacenes family, are considered as potential n-type semiconducting materials to be good alternatives to acenes for their electrondeficient nature, small band gaps and high thermal stabilities.[25, 29] In addition, they play an important role in fields such as photoinitiators,[30] chemical and biological Probe,[31-32] phosphorescent materials ligands[33] and organic crystalline materials.[34] The BP compounds were synthesized based on the cyclocondensation reactions between their respective 1,2-di aminoarenes precursors and phenanthrene-9,10-dione mixed with acetic acid and ethyl alcohol refluxing for 3h according to the previous literature (Scheme S1 in Electronic supplementary information).[25]

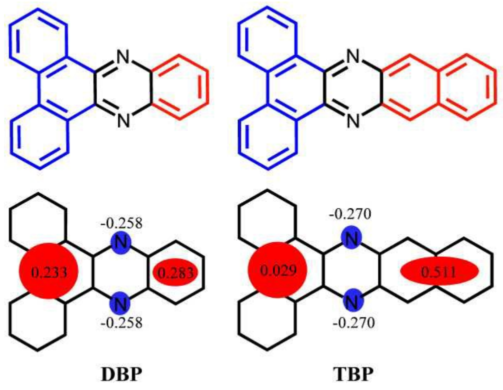

Fig. 1 Chemical structures (up) and Calculated charge distribution (bottom) by Gaussian 09 program for the ground states of dibenzo[a,c]phenazine (DBP) and tribenzo[a,c,i]phenazine (TBP).

The donor-acceptor-donor (D-A-D) structure based organic molecular have been shown to greatly enhance the ISC process both from previous experimental and theoretical researches.[35-38] As

View Article Online
DOI: 10.1039/C6NJ02747D

shown in Fig. 1, the introduction of two N atoms transforms the whole molecule skeleton to a D-A-D structure. As a result, the excitation process features an obvious charge-transfer character, which additionally reinforces the ISC process (vide infra).Fig. 2a and b depict the absorption spectra (black line), fluorescence spectra (red line) and phosphorescence spectra (blue line) of DBP and TBP in toluene (Tol) solution, respectively. Compared with DBP, spectra of TBP show obvious bathochromic shift due to the enlargement of the conjugated regions. In addition, the absorption spectra of TBP exhibit one more redundant weak peak at 473nm which demonstrates that the excitation progress of TBP is different from that of DBP.[39] Considering the different electronic structures between DBP and TBP as shown in Fig. 1, the strong absorption peak at 423 nm and the weak absorption peak at 473 nm for TBP may result from the strong charge-transfer from the naphthalene group to the pyrazine group (short as N-P transfer) and the negligible charge-transfer from the phenanthrene group to the pyrazine group (short as P-P transfer), respectively. Because of the approximately equal electron donating ability of the benzene group and the phenanthrene group in DBP, there is no abnormal difference on the intensity of absorption peak. This distinctly different charge-transfer induced excited states between DBP and TBP lead to their discriminative features of emission spectra.

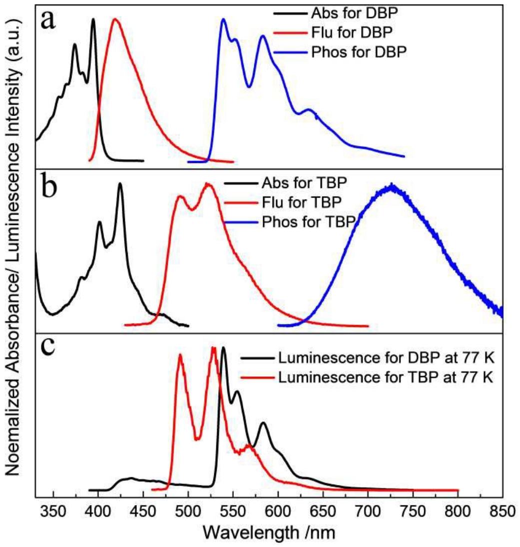

Fig. 2 (a) Normalized absorption spectra (black line), Fluorescence spectra (red line) and phosphorescence spectra (blue line) of DBP and (b) TBP in Toluene (Tol) dilute solution, respectively. The phosphorescence spectra were record at 77 K. (c) the luminescence spectra of DBP (black line) and TBP (red line) at 77 K.

In most case, for the reason that the luminescence spectra directly reflect the equilibrium excited state, luminescence spectra is considered to be an important tool to obtain the information about the electronic structure of the lowest excited state.[40] To further study the relationship between the CT characters and the emission features, the luminescence spectra which contain the fluorescence and phosphorescence information simultaneously for DBP (black line) and TBP (red line) were collected at 77 K as shown in Fig. 2c. We can see that DBP exhibits extremely stronger phosphorescence intensity at 539 nm with an absolute quantum efficiency of 8.45% than fluorescence at 419 nm with yield of 1.13% (Fig. S1 and Table 1). In contrast, TBP demonstrates almost no phosphorescence emission at 77 K accompanied by considerable fluorescence intensity at 492 nm with absolute efficiency of 7.07% (Fig. S1). However, singlet oxygen generation experiment (vide infra) using hypocrellin A (HA) as a standard reference (Φ_Δ=0.84 in Tol solution)[41] gives the high triplet yields of 77.1% and 58.7% for DBP and TBP as shown in Fig. 4 and Table 1, respectively. The discrepancy between the phosphorescence yields and triplet yields of DBP and TBP, both of which have high triplet yields but have distinctly different phosphorescence yields, demonstrates a possibly different fate for the CT-ISC produced triplet states between DBP and TBP. This may be related to the different kind of charge-transfer excited process between them.

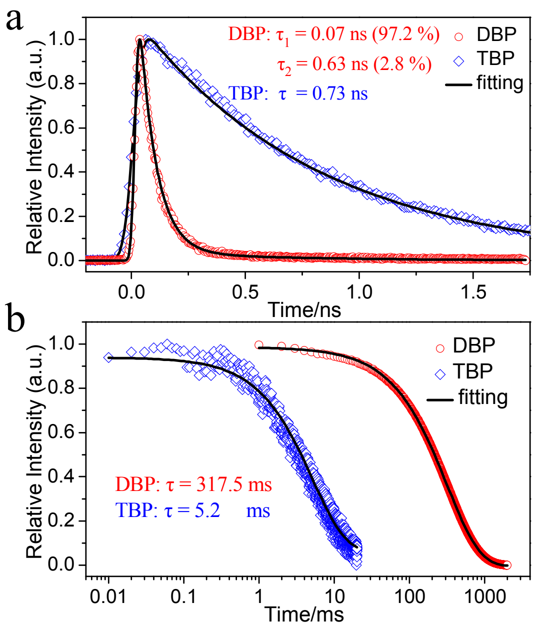

Fig. 3 (a) Time-resolved fluorescence spectra decay transient of DBP(red) and TBP (blue) in Tol dilute solution at room temperature with excitation wavelength of 400nm. (b) Phosphorescence spectra decay traces of DBP (red) and TBP (blue) in Tol dilute solution at 77 K with excitation wavelength of 400 nm. Note that the horizontal axils for (a) and (b) are linear and logarithmic, respectively.

3.2. Time-resolved luminescence kinetics

In order to investigate the low-lying excited states of singlet and triplet excited states for the BP compounds, time-resolved luminescence decay transient of DBP and TBP were measured in Tol dilute solution as shown in Fig. 3. The Fluorescence of DBP decays

View Article Online
DOI: 10.1039/C6NJ02747D

Table 1. Experimental and Calculated Optical Characteristics for the BP compounds.[a]

	Absorption			Emission					Phosphorescence				
	λ_{exp} / nm	λ_{cal} / nm	f	λ_{exp} / nm	λ_{cal} / nm	f	τ_F / ns	Φ_F / %	λ_{exp} / nm^b	λ_{cal} / nm	τ_P / ms^b	Φ_Δ / %	Φ_p / %^{b}
DBP	394	362	0.2385	419	377	0.2325	0.07 0.63	0.56 1.03^b	539	537	318	77.1	8.45
TBP	423 473	312 392	0.8025 0.2854	492	416	0.7564	0.73	0.67 7.07^b	722	823	5.2	58.7	<0.1

[a] The experimental data is extracted from the spectra in Tol solution at room-temperature if no special illustration. λ_{exp}= experimental symmetry-allowed lowest-lying absorption or emission wavelengths, λ_{calc}= calculated symmetry-allowed lowest-lying absorption or emission wavelengths, f = oscillator strengths, Φ_F = the quantum yield of fluorescence, Φ_p = the quantum yield of phosphorescence, Φ_T = triplet yield, τ_F =fluorescence lifetime, τ_P = phosphorescence lifetime. $_b$ measured at 77 K.

bi-exponentially which is dominated by short lifetime of 0.07 ns (97.2 %) accompanied with ignorable percent long lifetime of 0.63 ns (2.8 %) at room temperature. The time-resolved fluorescence spectra for DBP (Fig. S4) exhibits little difference between spectra integrated over 0.0 – 0.1 ns and 0.1 – 1.0 ns, which demonstrates that the two lifetime fluorescence result from the same excited state but produced by different processes. Considering the relative low phosphorescence yield for DBP compared with the high triplet yield (77.1 %), the longer lifetime fluorescence is probably attributed to the delayed fluorescence from the triplet state.[11, 19, 42] At the same time, the fluorescence of TBP follows a mono-exponential decay with lifetime of 0.73 ns, which is at the same timescale as the longer lifetime of DBP. The mono-exponentially decay of fluorescence, ~~and~~ the same excitation spectra for 490 nm and 524 nm (Fig. S2) and the same emission peaks with excitation wavelength of 420 nm and 470 nm (Fig. S3) demonstrate that the fluorescence of TBP derived from the same lowest lying singlet state. In addition, the high triplet yield (58.7 %), the almost negligible phosphorescence yield at 77K and the much higher fluorescence efficiency for TBP than DBP strongly suggest that fluorescence of TBP is the delayed fluorescence.

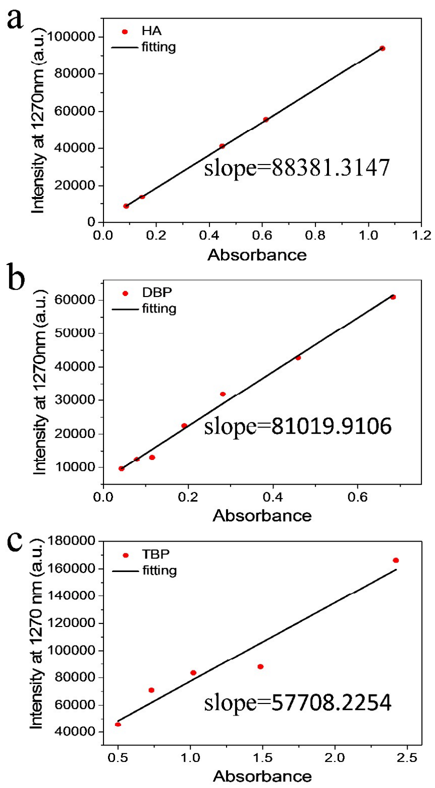

Fig.4 The luminescence intensity for singlet oxygen at 1270 nm as a function of absorbance for (a) hypocrellin A (HA), (b) DBP and (c) TBP in Tol solution at room temperature.

It should be emphasized that the "missing" of the normal fluorescence in TBP results from the high consumption of non-radiative transition process. We then performed the time-resolved fluorescence decay transient of DBP and TBP at 77 K (Fig. S5) to identify the delayed fluorescence. The fluorescence lifetime of DBP extents to 0.45 ns and 5.85 ns, respectively, with little percent change for the short and long lifetime compared with room temperature. However, the fluorescence of TBP follows bi-exponentially decays with lifetime of 0.78 ns and 10.02 ns. According to the lifetime of DBP at 77 K, lifetime of 0.78 ns is corresponding to the normal fluorescence and lifetime of 10.02 ns is corresponding to the delayed fluorescence. Compared with lifetime at room temperature, because of the restriction of non-radiative transition by temperature, the appearance of short lifetime fluorescence (which is attributed to the normal fluorescence) at 77 K further confirms the existence of delayed fluorescence. On

View Article Online
DOI: 10.1039/C6NJ02747D

the other hand, in contrast to fluorescence, lifetime for the phosphorescence of DBP extends to as long as 317.5 ms and is about two orders of magnitude longer than that of TBP with value of 5.2 ms at 77 K as shown in Fig. 3b. The magnitude difference between the lifetime of delayed fluorescence and phosphorescence illustrates the delayed fluorescence is probably not derived from the lowest triplet states T_1 but from higher energy level triplet states. In addition, the large ΔE_{ST} values (0.66 ev and 0.81 ev for DBP and TBP, respectively) make it almost impossible to conduct the reverse intersystem crossing process from the T_1 state to the S_1 state, which strongly support our opinion.

3.3. Singlet oxygen yield determination

The Φ_Δ value was measured by the singlet oxygen luminescent method using hypocrellin A (HA) as a standard reference (Φ_Δ=0.84 in Tol solution).[41] Triplet state whose energy is higher than that of triplet oxygen can transform the triplet oxygen to the singlet oxygen. Then, the singlet oxygen gives the 1270 nm emission upon returning to the triplet oxygen.[42] As a result, the amounts of triplet states are proportional to that of singlet oxygen and hence are proportional to the intensity of emission at 1270 nm.[43]

The singlet oxygen quantum yield (Φ_Δ) can be calculated using the following equation:[44]

$$\Phi_S = \Phi_R \cdot \frac{I_S/A_S}{I_R/A_R} = \Phi_R \cdot \frac{K_S}{K_R}$$

Where Φ is the singlet oxygen quantum yield, I is the intensity of the emission at 1270 nm, A is the corresponding absorbance, S and R refer to the sample and the reference, respectively. The luminescence intensity for singlet oxygen at 1270 nm as a function of the corresponding absorbance for (HA), DBP and TBP in Tol solution are shown in Fig. 4. The Φ_Δ values of DBP and TBP are 77.1 % and 58.7% , respectively, and are collected in Table 1. The high singlet oxygen yields strongly suggest high ISC efficiency exists in the BP compounds.

3.4. Femtosecond transient absorption spectra and data analysis

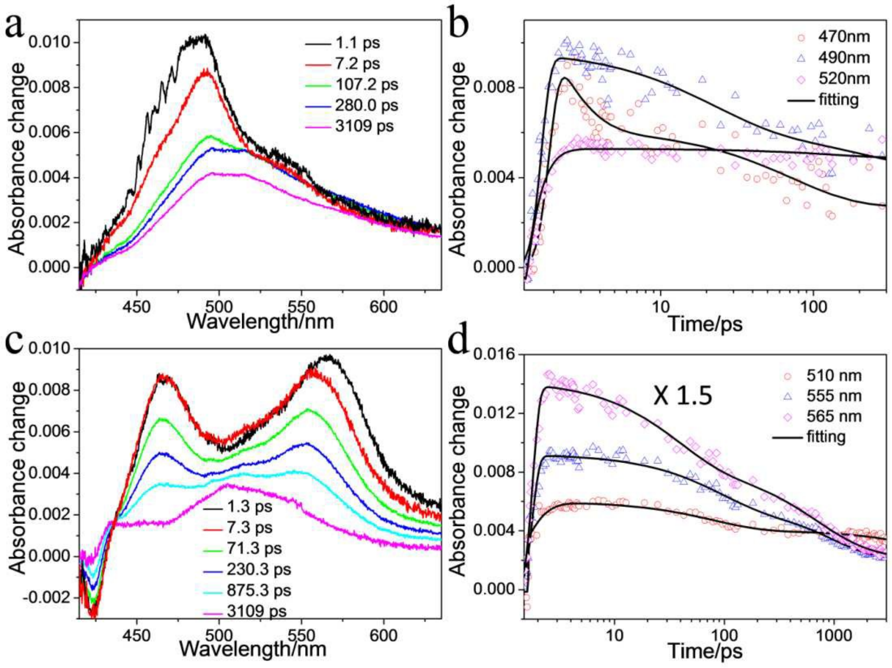

Fig. 5 (a) The femtosecond ultrafast transient absorption spectra of DBP and (c) TBP in TOL solution. (b) The kinetics traces (colored points) and fitting lines (black solid line) of DBP and (d) TBP (the kinetic of 565 nm was multiply by 1.5 to distinguish the kinetic of 555 nm) taken from the corresponding transient absorption spectra monitored at the absorption maxima of the transients. The pump laser wavelength is 400 nm.

To further confirm the above proposed photophysical process of the BP compounds, femtosecond transient absorption spectra were recorded in Tol solution with 400nm excitation of DBP (Fig. 5a) and TBP (Fig. 5c). Upon photoexcitation, both DBP and TBP exhibit abnormally fast excited-states dynamics characterized by a ~1 ps decay at ~ 470 nm for DBP and ~ 565 nm for TBP, respectively. We attribute this fast decay species to the vertical excitation high energy level singlet states S_n (vide infra). Meanwhile, analysis of ~ 520 nm for DBP and ~ 510 nm for TBP both produce one comparable rise time constant of ~ 1 ps and one long lifetime decay. This long lifetime specie is considered to be the triplet state and is

View Article Online
DOI: 10.1039/C6NJ02747D

further confirmed by the nanosecond flash photolysis experiments (Fig. S6). Apparently, the similar decay and rise time constants reveals a close correlation between the decay of the S_n state and the formation of the triplet state.[26] Combined the same charge-transfer characters for the singlet state and the triplet state of these BP compounds in the ISC process as shown in Fig. 6, the fast timescale demonstrates a charge-transfer induced ultrafast ISC process. This conclusion is in accordance with the high yield of triplet states for DBP and TBP as shown in Table 1 and Fig. 4. For DBP, the lowest lying singlet state S_1 follows a bi-exponential decay at ~ 490 nm with short lifetime of 75.8 ps and long lifetime of nanosecond level. The long lifetime decay species belongs to the triplet state on account of the big superposition bands between the absorption spectra of the singlet state and the triplet state. Due to this complicated superposition spectra and the negligible percent observed in the time-resolved fluorescence decay data, decay for the delayed fluorescence is not visible.

As to TBP, however, the lowest lying singlet state S_1 decays bi-exponentially with lifetime of 35.8 ps (22.7 %) and 675.6 ps (77.3 %) accompanied by the same absorption peaks at ~ 465 nm and ~ 555 nm. A nanosecond level decay was also observed at the same band for the triplet state as a result of the superposition absorption spectra of the singlet state and the triplet state. Apparently, we observe both the normal singlet state (35.8 ps) and the reverse ISC process produced singlet state (675.6 ps). For the minority of the normal singlet state and the high possibility of nonradiative transition in TBP, only the delayed fluorescence can be characterized by the time-resolved fluorescence experiment at room temperature as shown in Fig. 3a. The appearance of short lifetime decay for the fluorescence of TBP at 77 K confirms this opinion further (Fig. S5).

3.5 Theoretical calculations

Finally, we performed theoretical computational studies using TD-DFT methods at the B3LYP/6-311^{++}G** level to gain more insight on the photophysical mode of the BP compounds.[27-28] The BP molecular skeleton can be treated as a Donor-Acceptor-Donor (D-A-D) structure and has the C_{2v} symmetry with A_1 ground state. Therefore, the excitation process should be symmetry-preferential process.[45] Fig. 6 reproduces the TD-DFT-calculated energy levels, isosurface, symmetry and main orbital configurations of (a) DBP and (b) TBP at singlet (S_n) and triplet (T_n) states. For DBP, the lowest lying symmetry-allowed singlet excited state is the S_3 state, which is attributed to the charge transfer transition both from the phenanthrene group and the benzene group to the pyrazine group (Fig. 5a from the yellow part to the blue part for S_3) with oscillator strengths of $f = 0.2385$ (Table 1 and Table S1). Upon photoexcitation, owing to the symmetry restriction, the DBP molecular was excited to the S_3 state. Then the S_3 state undergoes the charge-transfer induced ultrafast ISC process to the high energy level triplet state T_n (T_2 and T_7 as shown in Fig. 6a). The large difference between the timescale of delayed fluorescence and phosphorescence illustrate the reverse ISC process is not from the T_1 state but from a higher energy level triplet state. The T_7 state can either transfer into the S_1 state via the reverse ISC process (RISC) or converts to the T_1 state via the internal conversion (IC) process. However, the large energy gap exists between the S_1 state and the T_2 state prevents the RISC process from the T_2 state. As a consequence, the only one reverse ISC route from T_7 to S_1 gives the negligible delayed fluorescence in DBP.

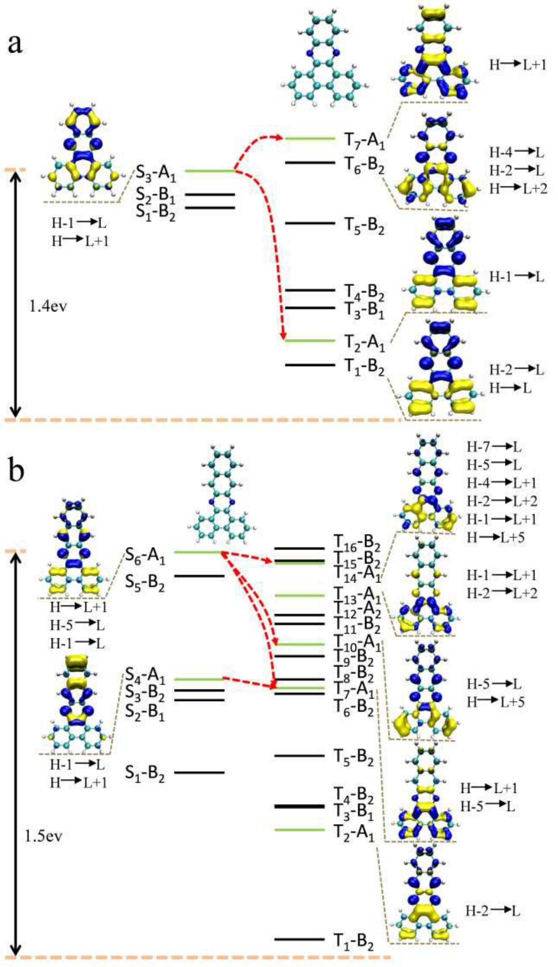

Fig. 6 Schematic diagrams showing the TD-DFT-calculated energy levels, isosurface, symmetry and main orbital configurations of (a) DBP and (b) TBP at singlet (S_n) and triplet (T_n) states. Note that H and L stand for the highest occupied molecular orbital and lowest unoccupied molecular orbital, respectively. The green lines refer to the energy level which is symmetry-allowed excited. The red lines refer to the intersystem crossing processes probably occurring from the S_n state to its higher- or lower-lying triplet states (T_n). It also should be noted that the orange dashed line is not the ground state energy level.

By contrast, the TBP molecule conducts a more complicated photophysical process. The different electron donating ability of the phenanthrene group and the naphthalene group in TBP results into two distinct charge-transfer features for the lowest two symmetry-allowed singlet excited states (S_4 and S_6) as shown in Fig. 6b. The S_4 state is tagged by the naphthalene to phenazine (N-P) transfer with oscillator strengths $f = 0.2854$ while the S_6 state is marked by the phenanthrene to phenazine (P-P) transfer with oscillator strengths $f = 0.8025$ (Table 1 and Table S2). These two excited states and their

View Article Online
DOI: 10.1039/C6NJ02747D

oscillator strengths perfectly consistent with the weak absorption peak at 473 nm and the strong absorption peak at 423 nm in Fig. 2b. For the much stronger oscillator strengths of the S_6 state than the S_4 state, most of the TBP molecules were excited to the S_6 state. Correspondingly, the T_n (T_2, T_7, T_{10}, T_{14}) state produced from this state via the CT-ISC process will be much higher in energy level. As a result, the increased number of RISC channels from the T_n state (T_7, T_{10}, T_{14}) in TBP to the S_1 state enhances the delayed fluorescence. Automatically, only the delayed fluorescence can be observed at room temperature with the high consumption of the S_1 state by nonradiative transition at room temperature. The high triplet yield and the negligible phosphorescence at 77 K further verify the high reverse ISC efficiency.

3.6 Kinetic model

Therefore, we propose the model for the tunable lifetime and yield of fluorescence and phosphorescence in the BP compounds and describe it in Fig. 6. For the restriction of symmetry, the BP compounds were firstly excited to higher energy level singlet states (S_n) instead of the S_1 state. The charge-transfer character of the S_n state enhances the ISC process and gives the high yields of high energy level triplet states (T_n) other than the T_1 state. Then the T_n state can decays into either the S_1 state via the RISC process and hence gives the delayed fluorescence or the T_1 state via the IC process. It should be noted that the more number of the T_n states produced by the CT-ISC process means the more channels of RISC process to the S_1 state. We can conclude directly from Fig. 6 that the energy gap between the firstly excited state S_n and the S_1 state (short as ΔE) greatly affects the number of T_n. As a result, the large ΔE value in TBP leads to the high efficiency RISC process which accounts for the long lifetime of fluorescence and the negligible phosphorescence. However, the small ΔE value in DBP vastly prevents the RISC process and gives the much stronger phosphorescence (8.45 %) than fluorescence (1.03%) for the high ISC efficiency. It is well known that the phosphorescence lifetime τ_P can be expressed by the following equation:[31-32]

$$\tau_P = \frac{\Phi_{ST}}{K_r + K_{nr} + K_{TS}} = \frac{\Phi_{ST} \cdot K_r}{\left(K_r + K_{nr} + K_{TS}\right) \cdot K_r} = \frac{\Phi_P}{K_r}$$

Where K_r and K_{nr} are the rate constants for radiative and nonradiative transition from the T_1 state, respectively, the K_{TS} is the rate constant for the RISC process from the triplet excitons to the singlet excitons, and the Φ_{ST} and Φ_P are the efficiency of the ISC process and phosphorescence emission, respectively. Typically, the K_r value is always 10^{-1} ~ 10^{-2} S^{-1} for hydrocarbon materials.[48-49] Therefore, large Φ_{ST} value and small K_{TS} value will contribute to forming the long-lasting phosphorescence. Consequently, it is reasonable to achieve long-lasting phosphorescence when strictly prevent the RISC process in high triplet yields material By this way, the high phosphorescence yield (8.45 %) in DBP gives the long-lasting phosphorescence (318 ms) than that of TBP (5.2 ms) with negligible phosphorescence yield (< 0.1 %).

Based on the strong phosphorescence for DBP in toluene solution at 77 K, we successfully observed the room temperature long-lasting phosphorescence in the crystal of DBP. Unfortunatelythis phenomenon can only be observed in few points among plenty of DBP crystals upon photoexcitation. We attributed it to crystal defect for the reason that DBP prefer to form twin crystal. Because of this, it is difficult for us to character the room temperature long-lasting phosphorescence of DBP, such as lifetime, spectra and photograph. Therefore, further experiments are required to completely realize the long-lasting room temperature phosphorescence in DBP crystal.

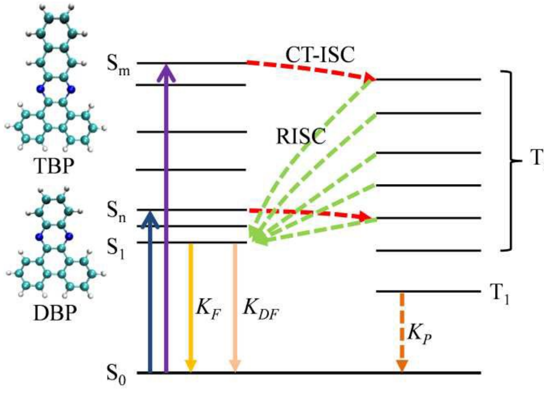

Fig. 7 Proposed mechanism for the photophysical process of the BP compounds.

4 Conclusions

In conclusion, we have synthesized two aza-acenes of dibenzo[a,c]phenazine (DBP) and tribenzo[a,c,i]phenazine (TBP) with C_{2v} symmetry and demonstrated the mechanism for the tunable lifetime and yield of fluorescence and phosphorescence. Because of the symmetry for the benzophenazine compounds, the excited states transition process is symmetry-controlled. Therefore, the BP compounds were firstly excited to the high energy level singlet state S_n instead of the S_1 state. Besides, the higher energy level S_n state will lead to the increased numbers of the T_n state via the intersystem crossing process, which in turn increase the channels of the reverse intersystem crossing process. As a consequence, considerable longer fluorescence lifetime due to the delayed fluorescence and negligible phosphorescence were observed. This is the situation in TBP though with high triplet yield produced by the charge-transfer induced ultrafast intersystem crossing (CT-ISC) process. In DBP, however, the weaker electron donating group results into the relative lower energy level S_n state upon photo-excitation, which greatly reduce the channels for the reverse intersystem crossing process. Accompanied with the high yield of triplets (77.0 %) produced by the charge-transfer induced ultrafast intersystem crossing (CT-ISC) process, DBP exhibits much stronger long-lasting phosphorescence (8.45 % yields and 317.5 ms) than fluorescence (1.03 %, 0.45 ns) at 77 K, which premise the achievement of long-lasting room temperature phosphorescence in the DBP crystal. This mechanism will be helpful in designing pure organic high triplet yields materials and high performance OLEDs materials.

DOI: 10.1039/C6NJ02747D

Acknowledgements

This work was supported by the National Natural Science Foundation of China (Nos. 21573251, 21521062, 21190034, and 21221002), project of the State Key Laboratory on Integrated Optoelectronics of Jilin University (IOSKL2014KF16), project of Construction of Innovative Teams and Teacher Career Development for Universities and Colleges Under Beijing Municipality (IDHT20140512), the National Basic Research Program of China (973) 2011CB808402, 2013CB933500, and the Chinese Academy of Sciences.

Notes and References

1 L. Xu, Y Li, S. Li, R. Hu, A. Qin, B. Z. Tang, B Su, *Analyst* 2014, **139,** 2332.
2 L. Yuan, W. Lin, K. Zheng, L. He, W Huang, *Chem. Soc. Rev.* 2013, **42,** 622-661.
3 G. Zhang, G. M. Palmer, M. W. Dewhirst, C. L Fraser, *Nat. Mater.* 2009, **8,** 747-751.
4 X. D. Wang, O. S. Wolfbeis, R. J Meier, *Chem. Soc. Rev.* 2013, **42,** 7834-7869.
5 P. R. N. Childs, J. R. Greenwood, C. A Long, *Rev. Sci. Instrum.* 2000 **71,** 2959.
6 X. Wang, Q. Liao, Q. Kong, Y. Zhang, Z. Xu, X. Lu, H Fu, *Angew. Chem. Int. Ed* 2014, **53,** 5863-5867.
7 X. Wang, H. Li, Y. Wu, Z. Xu, H. Fu, *J. Am. Chem. Soc.* 2014, **136,** 16602-16608.
8 X. Wang, Q. Liao, H. Li, S. Bai, Y. Wu, X. Lu, H. Hu, Q. Shi, H. Fu, J. *Am. Chem. Soc.* 2015, **137,** 9289-9295.
9 X. Wang, Q. Liao, X. Lu, H. Li, Z. Xu, H. Fu, *Sci. Rep.* 2014, **4,** 7011.
10 C. Murawski, K. Leo, M. C. Gather, *Adv. Mater.* 2013, **25,** 6801-6827.
11 H. Uoyama, K. Goushi, K. Shizu, H. Nomura, C. Adachi, *Nature* 2012, **492 ,** 234-238.
12 S. Mukherjee, P. Thilagar, *Chem. Commun.* 2015, **51,** 10988.
13 Y. Tao, C. Yang, J. Qin, *Chem. Soc. Rev.* 2011, **40,** 2943-2970.
14 R. Kabe, N. Notsuka, K. Yoshida, C. Adachi, *Adv. Mater.* 2016, **28,** 655-60.
15 S. Hoshino, H. Suzuki, *Appl. Phys. Lett.* 1996, **69,** 224.
16 H. Najafov, B. Lee, Q. Zhou, L. C. Feldman, V. Podzorov, *Nat. Mater.* 2010, **9,** 938-943.
17 D. Chaudhuri, E. Sigmund, A. Meyer, L. Rock, P. Klemm, S. Lautenschlager, A. Schmid, S. R. Yost, T. Van Voorhis, S. Bange, S. Hoger, J. M. Lupton, *Angew. Chem. Int. Ed.* 2013, **52,** 13449-13452.
18 A. Montes Victor, P.-B. C., Agarwal Neeraj, Shinar Joseph, Jr. Pavel Anzenbacher, *J. Am. Chem. Soc.* 2006, **128,** 12436-12438.
19 M. Segal, M. Singh, K. Rivoire, S. Difley, T. Van Voorhis, M. A. Baldo, *Nat. Mater.* 2007, **6,** 374-378.
20 D. Hu,L. Yao,B. Yang,Y. Ma, *Phil.Trans. R. Soc. A* 2015, **373**: 20140318.
21 K. Kikuchi, H. Fukumra, H. Kokubun, *Chem. Phys. Lett.* 1986, **123**, 226–228.
22 R. Redmond, I. Kochevar, M. Krieg, G. Smith, W. McGimpsey, *J. Phys. Chem. A* 1997, **101**, 2773–2777.
23 K. Tokumura, M. Kurauchi, O. Oyama, *J. Photochem. Photobiol. A* 1994, **81**, 151–158.
24 W. Li, Y. Pan, L. Yao, H. Liu, S. Zhang, C. Wang, F. Shen, P. Lu, B. Yang, Y. Ma, *Adv. Optical Mater.* 2014, **2**, 892-901.
25 P. K. Sahoo, C. Giri, T. S. Haldar, R. Puttreddy, K. Rissanen, P. Mal, *Eur. J. Org. Chem.* 2016, **7**, 1283-1291.
26 Y. Wu, K. Liu, H. Liu, Y. Zhang, H. Zhang, J. Yao, H. Fu, *J. Phys. Chem. Lett.* 2014, **5,** 3451-3455.
27 G. W. T. M. J. Frisch, H. B. Schlegel, G. E. Scuseria, M. A. Robb, J. R. Cheeseman, G. Scalmani, V. Barone, B. Mennucci, G. A. Petersson, H. Nakatsuji, M. Caricato, X. Li, H. P. Hratchian, A. F. Izmaylov, J. Bloino, G. Zheng, J. L. Sonnenberg, M. Hada, M. Ehara, K. Toyota, R. Fukuda, J. Hasegawa, M. Ishida, T. Nakajima, Y. Honda, O. Kitao, H. Nakai, T. Vreven, J. A. Montgomery, Jr., J. E. Peralta, F. Ogliaro, M. Bearpark, J. J. Heyd, E. Brothers, K. N. Kudin, V. N. Staroverov, R. Kobayashi, J. Normand, K. Raghavachari, A. Rendell, J. C. Burant, S. S. Iyengar, J. Tomasi, M. Cossi, N. Rega, J. M. Millam, M. Klene, J. E. Knox, J. B. Cross, V. Bakken, C. Adamo, J. Jaramillo, R. Gomperts, R. E. Stratmann, O. Yazyev, A. J. Austin, R. Cammi, C. Pomelli, J. W. Ochterski, R. L. Martin, K. Morokuma, V. G. Zakrzewski, G. A. Voth, P. Salvador, J. J. Dannenberg, S. Dapprich, A. D. Daniels, O. Farkas, J. B. Foresman, J. V. Ortiz, J. Cioslowski, and D. J. Fox, Gaussian, Inc., Wallingford CT, Gaussian 09, Revision **A.02**, 2009.
28 T. Lu, Multiwfn - A Multifunctional Wavefunction Analyzer. Multiwfn, Version **3.3.7** 2015.
29 L. Qiu, X. Zhuang, N. Zhao, X. Wang, Z. An, Z. Lan, X. Wan, *Chem. Commun.* 2014, **50**, 3324–3327.
30 Z. Kucybała, A. Kosobucka, *Polymer Bulletin* 2006, **56**, 321–329.
31 D. Dey, A. Bose, D. Bhattacharyya, S. Basu, S. S. Maity, S. Ghosh, *J. Phys. Chem. A* 2007, **42**, 10500-10506.
32 W. Guo, B. J. Engelman, T. L. Haywood, N. B. Blok, D. S. Beaudoin, S. O. Obare, *Talanta* 2011, **87**, 276–283.
33 T. Bura, P. Retailleau, M. T. Indelli, R. Ziessel, *Dalton Trans.* 2013, **42**, 4544.
34 A. Putta, J. D. Mottishaw, Z. Wang, H. Sun, *Cryst. Growth Des.* 2014, **14**, 350–356.
35 D. Veldman, S. Chopin, S. Meskers, R. Janssen, *J. Phys. Chem. A* 2008, **112**, 8617–8632.
36 Z. Dance, S. Mickley, T. Wilson, A. Ricks, A. Scott, M. Ratner, M. Wasielewski, *J. Phys. Chem. A* 2008, **112**, 4194-4201.
37 I. Gould, J. Boiani, E. Gaillard, J. Goodman, S. Farid, *J. Phys. Chem. A* 2003, **107**, 3515-3524.
38 M. Moral, L. Muccioli, W. Son, Y. Olivier, J. Sancho-García, *J. Chem. Theory Comput.* 2015, **11**, 168–177.
39 M. Kobayashi, N. Hayakawa, T. Matsuo, B. Li, T. Fukunaga, D. Hashizume, H. Fueno, K. Tanaka, K. Tamao, *J. Am. Chem. Soc.* 2016, **138,** 758-761.
40 N. Mataga, Y Murata, *J Am. Chem. Soc.* 1969, **91,** 3144-3152.
41 Z. Diwu, J. Lownt, *J. Photochem. Photobiol. A: Chem.* 1992, **64,** 273-287.
42 C. Sun, Q. Liao, T. Li, J. Li, J. Jiang, Z. Xu, X. Wang, R. Shen, D. Bai, Q. Wang, S. Zhang, H. Fu, H. Zhang, *Chem. Sci.* 2015, **6**, 761.
43 H. Yersin, A. F. Rausch, R. Czerwieniec, T. Hofbeck, T. Fischer, *Coordin. Chem. Rev.* 2011, **255,** 2622-2652.
44 Z. Yu, Y. Wu, Q. Peng,C. Sun, J. Chen, J. Yao and H. Fu, *Chem. Eur. J.* 2016, **22**, 4717-4722.
45 R. Han, Y. Wu, J. Feng, X. Ai, J. Zhang and L Skibsted *Photochem. Photobiol.* 2004, **80,** 326-333.

View Article Online
DOI: 10.1039/C6NJ02747D

46 Y. Gong, G. Chen, Q. Peng, W. Z. Yuan, Y. Xie, S. Li, Y. Zhang,; B. Z. Tang, *Adv. Mater.* 2015, **27,** 6195-6201.
47 M. S. Kwon, Y. Yu, C. Coburn, A. W. Phillips, K. Chung, A. Shanker, J. Jung, G. Kim, K. Pipe, S. R. Forrest, J. H. Youk, J. Gierschner, J. Kim, *Nat. Commun.* 2015, **6,** 8947.
48 A. Köhler, H. Bässler, *Sci. Eng. R* 2009, **66,** 71-109.
49 M. Gouterman, *J. Chem. Phys.* 1962, **36,** 2846.

View Article Online
DOI: 10.1039/C6NJ02747D

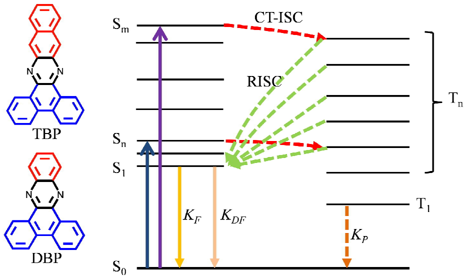

The enhanced charge-transfer interaction from DBP to TBP leads to higher energy triplet states, which reinforces the reverse intersystem crossing.